

Experimental and Numerical Approach to Investigate the Effect of Tool Geometry for EDM- Drilling

P. R. Vader¹, M.S. Nagrale², S. A. Mastud³

¹(Mechanical Engineering Department, Sardar Patel College of Engineering, Mumbai, India)

²(Mechanical Engineering Department, Sardar Patel College of Engineering, Mumbai, India)

³(Mechanical Engineering Department, Veermata Jijabai Technological Institute, Mumbai, India)

Abstract: Electrical discharge machining (EDM) has been used through decades in various industries like Medical, Defence, Aerospace etc. For EDM process different tool geometries are used such as a tubular and multi-channel. The study includes experimental analysis carried out by varying various process parameters voltage, current, pulse time, etc. on Micro-EDM machine. Material removed in EDM is due to spark erosion process. Finite element analysis (FEA) modelling of EDM will be carried out to predict the MRR. Gaussian heat flux distribution equation is used in the single spark calculation of MRR. The volume of material removed is calculated from the temperature distribution profile. From the study it was found that MRR for the multi-channel electrode is higher than tubular electrode in EDM-drilling. It offers high productivity in terms of MRR with significant time reduction. Industries can leverage this study for achieving productivity targets which in turn will reflect into tangible benefits. In this study single spark FEA analysis is performed followed by experimental validation.

Keywords: EDM, FEA, single spark, MRR, Tool Geometry.

I. Introduction

EDM is a non-conventional machining process in which electrical energy is converted into thermal energy. In EDM, the material is removed due to spark generation between anode and cathode electrode. Material removal depends on the properties like melting point, electrical resistivity, thermal conductivity, etc. Dielectric used for machining process performs two functions, acts as a conductor between tool electrode (anode) and workpiece (cathode) to control the spark gap and helps to flush debris present in the spark gap. Flushing of debris gives better MRR for the EDM process, but a portion of melted material re-solidifies during machining and forms crater. The efficiency of EDM depends on the material removal rate of the workpiece. As the input parameters such as current and voltage increases, MRR also increases. S. Jithin [1], suggested that assuming temperature dependent properties such as thermal conductivity and Gaussian heat flux equation, numerical simulation predicts the crater radius and can be compared with the experimental result. A. Okka [2] reported that the tubular electrode gives better performance than the multi-channel electrode. H. Singh [3] explained that the heat generated during spark is absorbed by workpiece. Numerical analysis is explained by S. Joshi [4] using three dimensional models of latent heat. Thermal analysis was carried out by using Gaussian heat flux as suggested by F. Zang [5]. Heat flux at workpiece depends on the spark radius, current and voltage. After applying the heat at workpiece, a crater is formed. This is explained by Sahu [6] using ANSYS software based analysis. P. Sharma [7] explained that, the input process parameters depend on material of electrode and workpiece.

II. Prerequisite For FEA Analysis

A FEA model is proposed to simulate EDM for single spark, and using aspects such as Gaussian heat flux distribution equation, variable spark radius and cathode energy fraction. As stated by S. Jithin, consideration of these aspects gives better results using FEA [1].

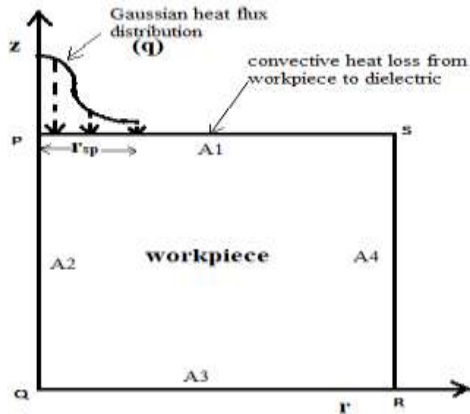
Assumption during numerical analysis:

- Workpiece material is homogeneous and isotropic.
- Ambient temperature is considered as 297K.
- Flushing efficiency is considered as 100%.
- The fraction of energy is depending on the 'pulse on time'.
- Simulation is done for single spark.

For this FEA analysis Fourier heat conduction equation is used as governing equation, as follows [4]:

$$\frac{1}{r} \frac{\partial}{\partial r} \left(K_t r \frac{\partial T}{\partial r} \right) + \frac{\partial}{\partial z} \left(K_t \frac{\partial T}{\partial z} \right) = \rho C_p \frac{\partial T}{\partial t} \quad (1)$$

where, r and z are cylindrical coordinates, K_t is thermal conductivity, C_p is specific heat, ρ is density, T and t are temperature and time respectively. Material properties are depending on the temperature and analysis can be done for a single spark. The Fig. 1 shows the axisymmetric thermal model of EDM. PQRS shows workpiece which is submerged in dielectric fluid [5]. In Fig.1 A1, A2, A3, and A4 show boundaries of a workpiece. Boundaries A2, A3, and A4 are far away from the axis of symmetry so the boundaries are assumed to be insulated ($\partial T/\partial z=0$) [5]. Therefore boundary conditions for A1 is shown in equation (2) [1],



$$K_t \frac{\partial T}{\partial z} = \begin{cases} q, & r < r_{sp} \\ h(T - T_0), & r > r_{sp} \\ 0, & t > t_{on} \end{cases} \quad (2)$$

Fig. 1: Gaussian heat distribution model

Using Gaussian heat flux distribution, for this numerical analysis equation [4] is given as:

$$q = \frac{4.45 * F_c IV}{\pi(r_{sp})^2} * e^{(-4.5 * \left[\frac{R}{r_{sp}}\right]^2)} \quad (3)$$

In these heat flux equation where F_c is the fraction of energy at a cathode, I is current in Ampere, V is applied voltage in Volt, r_{sp} is a spark radius and R is a radial distance from spark centre. Spark radius depends on applied input voltage and capacitance [6]. Using experimental methods, it is very difficult to find spark radius at heat source for single spark conditions. This is because of pulse on time [1]. All generated heat is not conducted through workpiece so, the fraction of energy at the cathode is considered in account of convection losses in heat calculation and it depends on energy released due to the single spark (E) the workpiece [1]. This is given by:

$$E = I * V * T_{on} \quad (4)$$

Value of fraction of energy at the cathode (F_c) depends on current, applied voltage and pulse on time [7]. So the value of F_c is selected from the spark energy value [1] given by:

$$F_c = \begin{cases} 0.109 \text{ if, } E = 0 - 50mj \\ 0.187 \text{ if, } E = 50 - 100mj \\ 0.256 \text{ if, } E > 100mj \end{cases} \quad (5)$$

III. FEA Modelling And Process Flow

1. FEA model

Numerical analysis performed by using "ANSYS 16.0" software by using transient thermal analysis. An analysis was performed on brass workpiece. For this analysis, a 2D rectangular model was used with 5 μ m height, 20 μ m width and element size of 0.2 μ m. Selection of smaller element size gives better crater size [1]. Thermal properties of brass material are given below in Table 1,

Table 1: Workpiece material properties

Thermal conductivity(W/mK)	115
Specific heat(J/Kg K)	380
Density(Kg/m ³)	8600
Melting point(⁰ C)	940

2. FEA Steps

For this analysis Thermal h method was selected, after this select element type. Create geometry as per the specifications and material properties are to be applied. After completing geometry select proper mesh for the geometry by varying mesh size. For this geometry apply all boundary condition to plot result. For material removal, assign melting temperature. The elements having the temperature above melting point are killed. The detailed steps for FEA are shown in Fig.2,

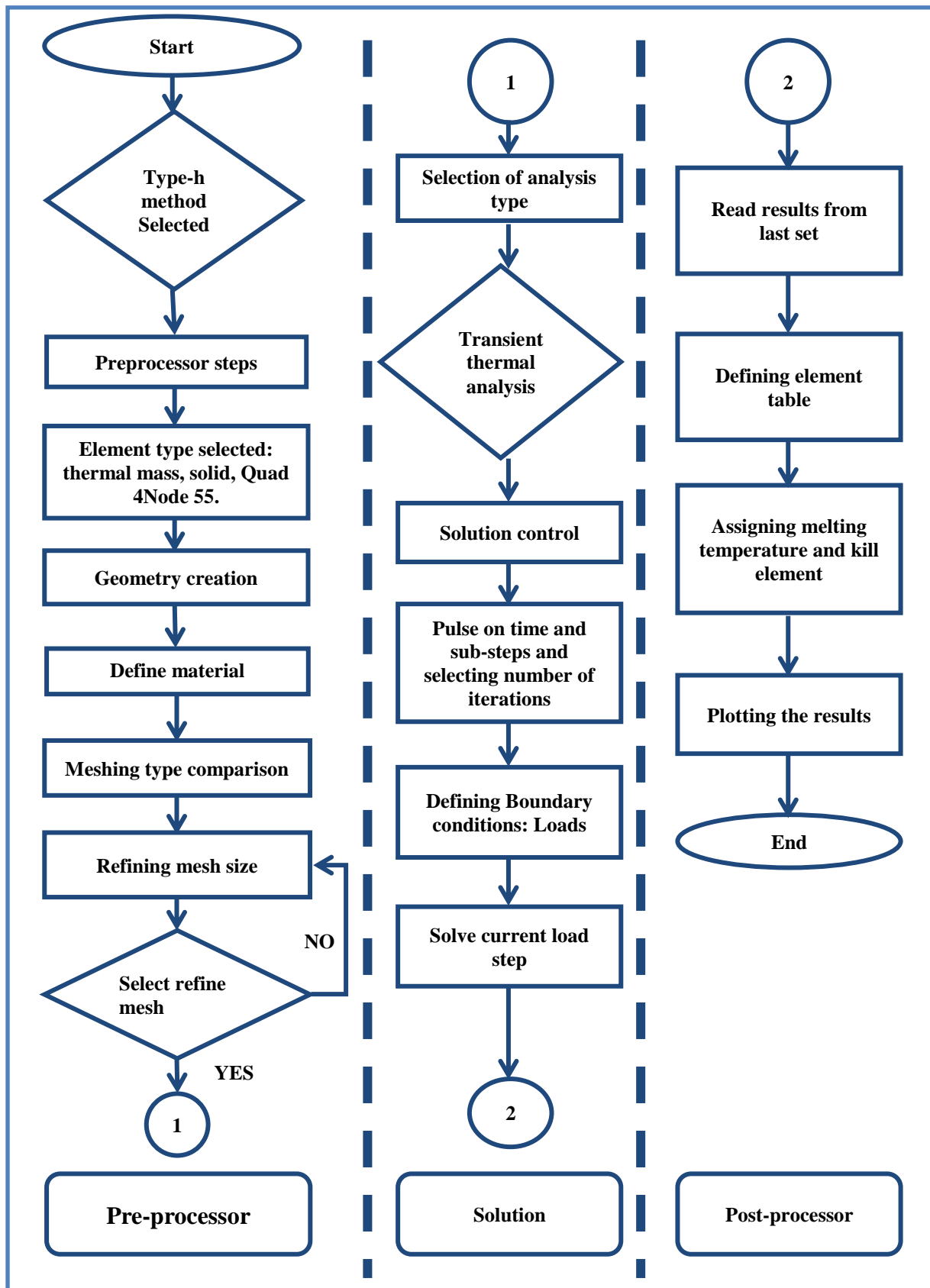


Fig.2. FEA Process Architecture

3. Input Conditions

FEA performed for different input condition are listed below in Table 2. For explanation of boundary conditions refer Fig.1. Value of heat flux is calculated from the above equation(3) by using equations(4) and equation(5). Value of cathode energy fraction F_c is selected as 0.109 using equation (5) [1].

Table 2: Input Parameter

Sr. No.	Voltage (V)	Current (A)	Spark radius(μm)	Heat flux $^W/m^2\text{ }^\circ\text{C}$
1.	100	0.1	48.27	679371141.6
2.	125	0.125	54.47	833617778.1
3.	150	0.15	60.67	967600804.4

Finite element analysis was performed for maximum heat flux, so heat is applied at origin node as shown in Fig.3. For this analysis, Convection is applied at workpiece and dielectric interface i.e.at the top surface of the model with convective heat transfer coefficient of $9000\text{ }^W/m^2\text{ }^\circ\text{C}$ as shown in

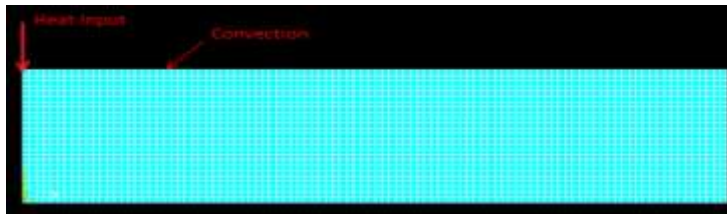


Fig. 3: ANSYS loading diagram

4. MRR Analysis

Crater formed after removal of melted element of material is analogous to the cylindrical circular discs as shown in Fig.4[4]. The material removal rate is calculated for machining time of $20\mu\text{s}$ i.e. ($t_{on} + t_{off}$)[8]. Formula for calculating crater volume is shown in equation (6) and MRR calculated from equation (7).

$$crater\ volume(mm^3) = \pi \sum_{1}^n R_n^2 t \tag{6}$$

$$MRR = \frac{crater\ volume\ obtained\ for\ single\ spark(mm^3) * 60}{(t_{on} + t_{off})(sec)} \tag{7}$$

Where R is the radius of the disc, t is the thickness of the disc which is equal to mesh size of element.

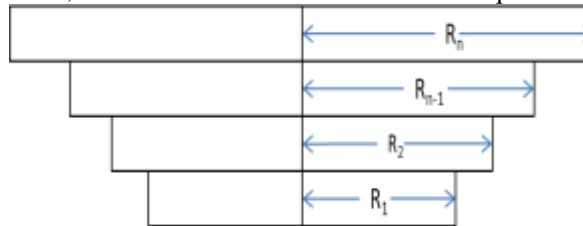


Fig. 4: Crater Volume

5. MRR Contours applying FEA

Following figures shows the results obtained after application of boundary conditions. In which Fig.5 (a) depicts a sample of temperature distribution after applying heat flux. The Fig.5 (b), (c) &(d) shows crater formed for the different input loading cases as mentioned below figures. From this analysis, it seems that with increase in heat flux, MRR value also increases. Results which are obtained from the analysis are listed in the Table 3.

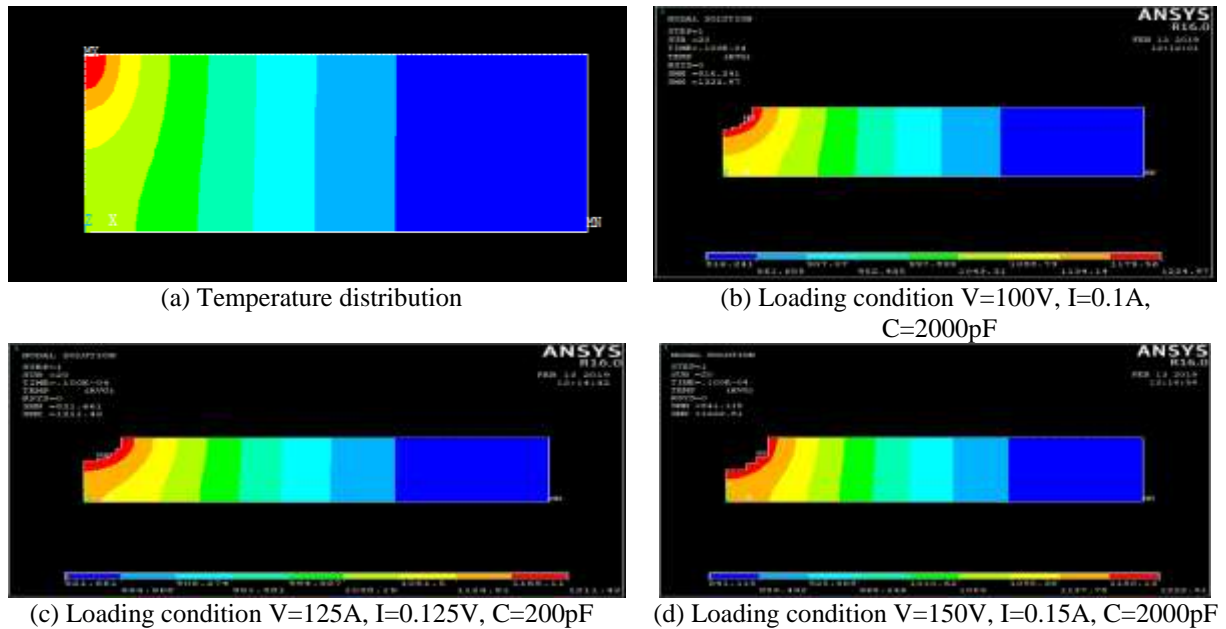


Fig. 5: MRR Contours applying FEA

Table 3: ANSYS FEA results

Sr.No.	Current(A)	Voltage(V)	Capacitance(pF)	MRR(mm^3/min)
1.	0.1	100	2000	0.03438
2.	0.125	125	2000	0.0942
3.	0.15	150	2000	0.143727

IV. Experimental Analysis

This section describes preliminary experiments that were performed for finding MRR using different tool geometries. Experiments were carried out on Hyper-15 tabletop type miniature Micro-EDM machine as shown in the Fig.6. For this analysis, brass is used as the workpiece. Brass material for the workpiece was selected in this experiment based on the parameters such as good electrical conductivity, machinability, etc. Copper electrode having tubular and multi-channel with an outer diameter 1mm is used for machining. Machining was carried out for the different spindle speed. For experimental analysis Total fina EDM oil 3 used as a dielectric fluid for machining.



Fig. 6: Hyper-15 Table Top Micro-EDM

Input conditions for which experiments were carried out are as shown in Table 4.

Table 4: Experimental input conditions

Voltage (V)	100, 125, 150
Current (Amp)	0.1, 0.125, 0.15
Capacitance (pF)	2000

For machining, workpiece used is of size 50*50*2.2 mm³. Workpiece material, tool material and dielectric used for machining are listed in Table 5 as given below,

Table 5: Material details for workpiece, tool and dielectric

workpiece	Brass
Tool Electrode	Copper electrode with tubular and Multi-channel
Dielectric fluid	Total fina EDM oil 3

For experimentation workpiece and tool electrode used are shown in Fig.7 given below. Fig.(a) shows brass workpiece used for experiment. Fig. (b) shows multi-channel copper electrode and Fig. (c) shows tubular copper electrode.

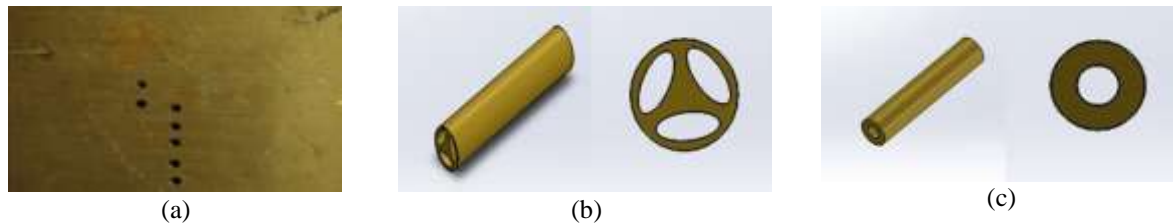


Fig.7: workpiece and tool electrode

1. MRR Calculation

The experiment was performed as explained earlier and the amount of material removed for the overall machining time was obtained. The MRR can be calculated using a relation as shown below,

$$MRR = \frac{\text{Volume of material removed}}{\text{Total machining time}} \quad (8)$$

Removed volume of material calculated from formula as shown in equation (9),

$$\text{volume of material removed} = \frac{\pi D_m^2 * L}{4} \quad \text{where, } D_m = \frac{d_1 + d_2}{2} \quad (9)$$

where,

D_m is mean diameter

d₁= Diameter of hole on upper surface

d₂= Diameter of hole on lower surface

L= Thickness of workpiece

2. Results and Discussion

Results obtained from experiments are as listed below in Table 6. It can be seen from the results that as input voltage increases, output MRR value is also increased in both cases. Flushing is the most important factor in EDM, in case of improper flushing; the debris in the gap may get re-solidify [2]. As seen in the results, MRR for a multi-channel electrode is more than tubular electrode for the same input conditions. Due to the effect of flushing, the MRR for the tubular electrode is lower than the multi-channel electrode. The results are as stated in Table 6.

Table 6: Results of Experiment

Sr. No.	Voltage(V)	Current(I)	Capacitance(pF)	Spindle speed (rpm)	MRR for tubular electrode(mm ³ /min)	MRR for multi-channel electrode
1.	100	0.1	2000	900	0.024	0.032
2.	125	0.125	2000	600	0.129	0.089
3.	150	0.15	2000	300	0.11	0.139

3. Validation of results

The comparison of experimental and FEA results are carried out. As MRR for the multi-channel electrode is more than tubular electrode for the same input condition. For this validation, only maximum MRR value is compared with FEA values. After Experimentation, MRR for a multi-channel electrode having input voltage 100V, 125V and 150V are respectively 0.032mm³/min, 0.089mm³/min and 0.139 mm³/min. During comparison experimental and FEA results, errors observed were 7.4%, 5.8%, and 3.4% as shown in Table 7.

Table 7: Comparison and %Error

Sr.no.	Expt. MRR Result for multi-channel electrode(mm ³ /min)	FEA MRR results (mm ³ /min)	% Error multi-channel electrode
1.	0.032	0.03438	7.4
2.	0.089	0.0942	5.8
3.	0.139	0.143727	3.4

V. Conclusion

The research was conducted to compare MRR results for multi-channel and tubular electrode. The analysis of the process is done using FEA methods backed by experimentations carried out on EDM. With regard to the above discussion and analysis results, it can be concluded that,

- From experiment, it is observed that as input conditions increase e.g. current, voltage, etc. MRR value also increases for both electrodes.
- MRR for the multi-channel electrode is more than tubular electrode; this difference is because of the flushing efficiency of EDM.
- During validation the average percentage error between the analytical and experimental observed value of MRR as 5.52%.

Acknowledgements

We would like to thank TEQIP III for the support during research and publication. Sincerely thanks to the “Production department, VJTI, Mumbai” for providing the experimentation facility.

Conflict of interest the authors declare that there is no conflict of interests regarding the publication of this paper.

References

- [1]. Jithin, S., Raut, A., Bhandarkar, U. V., & Joshi, S. S. FE Modeling for Single Spark in EDM Considering Plasma Flushing Efficiency. *Procedia Manufacturing*, 26, 2018, 617-628.
- [2]. Yilmaz, O., & Okka, M. A. Effect of single and multi-channel electrodes application on EDM fast hole drilling performance. *The International Journal of Advanced Manufacturing Technology*, 51(1-4), 2010, 185-194.
- [3]. Singh, H. Experimental study of distribution of energy during EDM process for utilization in thermal models. *International Journal of Heat and Mass Transfer*, 55(19-20), 2012, 5053-5064.
- [4]. Joshi, S. N., & Pande, S. S. Thermo-physical modeling of die-sinking EDM process. *Journal of manufacturing processes*, 12(1), 2010, 45-56.
- [5]. Zhang, F., Gu, L., & Zhao, W. Study of the Gaussian distribution of heat flux for micro-EDM. In *ASME 2015 International Manufacturing Science and Engineering Conference American Society of Mechanical Engineers*, 2015, V001T02A024-V001T02A024.
- [6]. Mohanty, C. P., Sahu, J., & Mahapatra, S. S. Thermal-structural analysis of electrical discharge machining process. *Procedia Engineering*, 51, 2013, 508-513.
- [7]. Sharma, P., Singh, S., & Mishra, D. R. Electrical discharge machining of AISI 329 stainless steel using copper and brass rotary tubular electrode. *Procedia Materials Science*, 5, 2014, 1771-1780.
- [8]. Mathew, J., Allesu, K., Srisailam, S., Somashekhar, K. P., & Suvin, P. S. Estimation of Residual Stresses and Crater Shape in μ -EDM by Finite Element Method. In *ASME 2012 International Mechanical Engineering Congress and Exposition American Society of Mechanical Engineers*, 2012, 1043-1046.